

# Kinetic and Equilibrium Binding Analysis of Protein–Ligand Interactions at Poly(amidoamine) Dendrimer Monolayers

Mi-Young Hong, Dohoon Lee, and Hak-Sung Kim\*

Department of Biological Sciences, Korea Advanced Institute of Science and Technology, 373-1 Kusung-dong, Yuseong-ku, Taejeon 305-701, Korea

The interaction of streptavidin (SA) with a biotinylated surface has been of great interest in the development of an interfacial layer for protein immobilization based on self-assembled monolayers (SAMs) and polymeric layers. Here, we demonstrate the unique characteristics of protein–ligand interactions on dendrimer monolayers based on kinetic and equilibrium binding analyses. With amine-ended poly(amidoamine) dendrimers from the first (G1) to fourth (G4) generation, the formation of even, compact dendrimer monolayers on gold was confirmed using FT-IR spectroscopy and ellipsometry. For the SA–biotin interaction, quantitative analysis of bound SA using surface plasmon resonance showed that the saturation binding level of SA was fairly higher in all dendrimer layers when compared to other tested systems of 11-mercaptopundecylamine SAMs and a poly(L-lysine) layer. Kinetic studies revealed that the initial binding rate of SA up to the saturation level was 2-fold higher in all dendrimer layers than in the SAMs regardless of the surface density of functionalized biotin. Concurrently, the dendrimer layers led to much higher values of sticking probability, which is defined as the probability that the SA molecule adsorbs upon collision with a biotinylated surface, at a fixed SA coverage, and prolonged the significant levels around the maximum probability with increasing SA coverage. Plots of the saturation coverage of SA versus the SA concentration in solution showed that SA binding onto the biotinylated G1 and G3 layers fit to a Langmuir isotherm model. Taken together, faster binding of SA and highly ordered packing of the molecules seems to be achieved through typical properties of the dendrimer monolayers such as surface distribution of functionalized biotin, surface corrugation, and flexibility of highly branched larger dendrimers, which provides a guideline for the construction and analysis of an interfacial layer in biosensing applications.

The interface for immobilization of biomolecules on a solid surface should fulfill the necessities that the biomolecules are efficiently immobilized in a molecularly organized manner without the loss of biological activity and with the minimization of

nonspecific adsorption of protein or cell debris. The surfaces immobilized or patterned with biomolecules have been widely applied to the simultaneous detection of diverse biospecific interactions in (multi-)biosensors and microarrays, complying with the growing demands from pharmaceutical, diagnostic, and biomedical areas. To increase the efficiency and sensitivity of biospecific interactions, much attention has been paid to the development of an interfacial layer enabling the immobilization of biomolecules in a controlled orientation and with minimized lateral steric hindrance.<sup>1</sup> These approaches have popularly employed the protein–ligand interaction of a streptavidin (SA)–biotin couple as the generic system to investigate the biospecific interactions on surfaces including self-assembled monolayers (SAMs),<sup>2–5</sup> dendrimer monolayers,<sup>6,7</sup> and entangled polymeric layers.<sup>8</sup> By the manipulation of biotin-containing mixed SAMs on gold, the protein–ligand interaction has been extensively studied in terms of adsorption kinetics and surface coverage of SA as a

- (1) (a) Ostuni, E.; Yan, L.; Whitesides, G. M. *Colloids Surf. B* **1999**, *15*, 3–30. (b) Brockman, J. M.; Frutos, A. G.; Corn, R. M. *J. Am. Chem. Soc.* **1999**, *121*, 8044–8051. (c) Houseman, B. T.; Gawalt, E. S.; Mrksich, M. *Langmuir* **2003**, *19*, 1522–1531. (d) Pavlickova, P.; Lensen, N. M.; Paul, H.; Schaeferling, M.; Giammasi, C.; Kruschina, M.; Du, W. D.; Theisen, M.; Ibba, M.; Ortigao, F.; Kambhampati, D. *J. J. Proteome Res.* **2002**, *1*, 227–231. (e) Frederix, F.; Bonroy, K.; Laureyn, W.; Reekmans, G.; Campitelli, A.; Dehaen, W.; Maes, G. *Langmuir* **2003**, *19*, 4351–4357. (f) Peluso, P.; Wilson, D. S.; Do, D.; Tran, H.; Venkatasubbaiah, M.; Quincy, D.; Heidecker, B.; Poindexter, K.; Tolani, N.; Phelan, M.; Witte, K.; Jung, L. S.; Wagner, P.; Nock, S. *Anal. Biochem.* **2003**, *312*, 113–124.
- (2) (a) Jung, L. S.; Nelson, K. E.; Stayton, P. S.; Campbell, C. T. *Langmuir* **2000**, *16*, 9421–9432. (b) Pérez-Luna, V. H.; O'Brien, M. J.; Opperman, K. A.; Hampton, P. D.; López, G. P.; Klumb, L. A.; Stayton, P. S. *J. Am. Chem. Soc.* **1999**, *121*, 6469–6478. (c) Spinke, J.; Liley, M.; Schmitt, F.-J.; Guder, H.-J.; Angermaier, L.; Knoll, W. *J. Chem. Phys.* **1993**, *99*, 7012–7019.
- (3) Ladd, J.; Boozer, C.; Yu, Q.; Chen, S.; Homola, J.; Jiang, S. *Langmuir* **2004**, *20*, 8090–8095.
- (4) Riepl, M.; Enander, K.; Liedberg, B.; Schäferling, M.; Kruschina, M.; Ortigao, F. *Langmuir* **2002**, *18*, 7016–7023.
- (5) Nelson, K. E.; Gamble, L.; Jung, L. S.; Boeckl, M. S.; Naeemi, E.; Golledge, S. L.; Sasaki, T.; Castner, D. G.; Campbell, C. T.; Stayton, P. S. *Langmuir* **2001**, *17*, 2807–2816.
- (6) Hong, M.-Y.; Yoon, H. C.; Kim H.-S. *Langmuir* **2003**, *19*, 416–421.
- (7) (a) Yang, M.; Tsang, E. M. W.; Wang, Y. A.; Peng, X. G.; Yu, H. Z. *Langmuir* **2005**, *21*, 1858–1865. (b) Pathak, S.; Singh, A. K.; McElhanon, J. R.; Dentinger, P. M. *Langmuir* **2004**, *20*, 6075–6079. (c) Anzai, J.; Kobayashi, Y.; Kakamura, N.; Nishimura, M.; Hoshi, T. *Langmuir* **1999**, *15*, 221–226.
- (8) (a) Frey, B. L.; Jordan, C. E.; Kornguth, S.; Corn, R. M. *Anal. Chem.* **1995**, *67*, 4452–4457. (b) Huang, N.-P.; Vörös, J.; De Paul, S. M.; Textor, M.; Spencer, N. D. *Langmuir* **2002**, *18*, 220–230. (c) Ruiz-Taylor, L. A.; Martin, T. L.; Wagner, P. *Langmuir* **2001**, *17*, 7313–7322. (d) Hobbs, S. K.; Shi, G.; Bednarski, M. D. *Bioconjugate Chem.* **2003**, *14*, 526–531.

\* Corresponding author. Phone: 82-42-869-2616. Fax: 82-42-869-2610. E-mail: hskim76@kaist.ac.kr.

function of the surface mole fraction of biotin ligands.<sup>2,5</sup> Dendrimer molecules have attracted great attention as a building block of nanostructures and biosensing interfaces<sup>9–11</sup> due to their extraordinary structural properties. These structural features include a precise molecular organization and a defined number of terminal groups for each generation, radially emanated and regularly concentrated chain-end groups from and around a central core of the molecule, and spherical shape the molecules attain at higher generations.<sup>12</sup>

Previously, we found that the monolayer of a fourth-generation (G4) poly(amidoamine) (PAMAM) dendrimer induces an efficient interaction of (strept)-avidin onto its biotinylated surface, resulting in an avidin binding level of  $\sim 5.0 \pm 0.2 \text{ ng}\cdot\text{mm}^{-2}$ .<sup>6</sup> The observed amount of bound avidin accounts for  $87 \pm 4\%$  surface coverage of protein, featuring packing of the molecules in a hexagonal arrangement, which is a theoretically attainable maximum level. Meanwhile, most of the biotin-containing SAMs were reported to result in the optimum level of  $\sim 2.4 \text{ ng}\cdot\text{mm}^{-2}$  for the interaction of SA.<sup>2–5</sup> Several approaches have shown that a dendrimer-coated surface as an interfacial layer renders high spatial densities for immobilization of probe molecules and, consequently, the enhanced capturing capacity of binding partners. These assets have broadened the implementation of the dendrimer layers for the fabrication of microarrays composed of DNA, protein, and antibody, enabling signal amplification for detection of DNA hybridization and quantitative assays with a substantially lowered detection limit and signal variation.<sup>11</sup>

In the present study, we report the unique characteristics of protein–ligand interactions on dendrimer monolayers based on kinetic and equilibrium binding analyses. As interfacial layers with different surface structures, PAMAM dendrimers from the first (G1) to G4 generation were employed for the construction of dendrimer monolayers on gold, and mixed SAMs and a poly(L-lysine) (PLL) layer were tested for comparison. Binding kinetics and equilibrium binding levels of SA on the biotinylated surfaces were determined using surface plasmon resonance (SPR), and the sticking probability of SA was analyzed with respect to the surface coverage of the molecule. The adsorption behavior of SA was predicted by fitting the observed data from binding isotherms of SA to a Langmuir isotherm model. Unique structural properties of the dendrimer monolayers were demonstrated by comparison with other tested layers in terms of the factors affecting the binding efficiency, such as surface distribution of ligands, surface corrugation, and flexibility of highly branched larger dendrimers. Details are reported herein.

## EXPERIMENTAL SECTION

**Materials.** Amine-ended starburst PAMAM dendrimers from G1 to G4, 11-mercaptoundecanoic acid (11-MUA), 11-mercaptoundecanol (11-MU-ol), 4-nitrobenzaldehyde (4-NB), and pentafluorophenol (PF<sub>5</sub>) were purchased from Aldrich. PLL with a molecular mass of 4–15 kDa, 1-ethyl-3-(3-dimethylaminopropyl) carbodiimide hydrochloride (EDAC), biotinyl- $\epsilon$ -amidocaproic acid *N*-hydroxysulfosuccinimide ester (sulfo-NHS-biotin), and SA were obtained from Sigma. 11-Mercaptoundecylamine (11-MUAmine) was purchased from Dojindo Laboratories. These reagents were used as received. All reagents used were purchased from conventional sources and were of the highest quality available. Doubly distilled and deionized water was used throughout the work. For the buffer solution, phosphate-buffered saline (10 mM phosphate, 17 mM KCl, and 138 mM NaCl) containing 0.05% Tween 20 (PBST, pH 7.4) was used.

**Preparation of Interfacial Layers on Gold.** The monolayers of PAMAM dendrimers and PLLs were constructed on gold according to the bottom-up synthetic procedures previously used by Crooks and our groups (Scheme 1).<sup>6,10b,13</sup> A gold substrate was freshly prepared through electron beam evaporation of Ti (2 nm) and then Au (40 nm) onto a Si[100] wafer. The gold-coated surface was cleaned with piranha solution (1:4 = 30% H<sub>2</sub>O<sub>2</sub>:concentrated H<sub>2</sub>SO<sub>4</sub> (v/v)) for 30 min. (CAUTION: Piranha solution reacts violently with most organic materials and must be handled with extreme care.) The cleaned gold surface was then chemisorbed with 11-MUA (2 mM in ethanol) for 2 h and subsequently activated with a solution of EDAC (100 mM) and PF<sub>5</sub> (200 mM) dissolved in DMF for 30 min. Activated 11-MUA SAMs presenting amine-reactive ester groups were covalently attached with amine-terminated PAMAM dendrimers and PLLs, respectively. In this case, the reaction solutions of PAMAM dendrimers from G1 to G4 were prepared at the same concentration of  $\sim 22 \text{ mM}$  (based on the number of primary amine terminal groups). PLL molecules were dissolved in 50 mM triethanolamine buffer (pH 8.0) containing 0.25 M NaCl to make a final concentration of  $\sim 2 \text{ mg/mL}$ . As stated by Frey and Corn, the significant amount of NaCl allows PLLs to overcome the electrostatic repulsion of ammonium groups and thereby form a complete and single monolayer.<sup>14</sup> After the coupling reaction for 2 h, the chemically modified substrate was immersed in a NaOH solution (10 mM, pH  $\sim 12$ ) for 30 min to remove remaining reactive groups. Following a thorough rinse with distilled water, the dendrimer-layered surface was transferred for further surface analysis.

Amine-presenting SAMs were prepared by chemisorbing 11-MUAmine (2 mM in ethanol) onto a cleaned gold surface for 24 h. The surface concentration of amine groups was controlled by varying the ratio of 11-MUAmine to 11-MU-ol in the reaction solution.

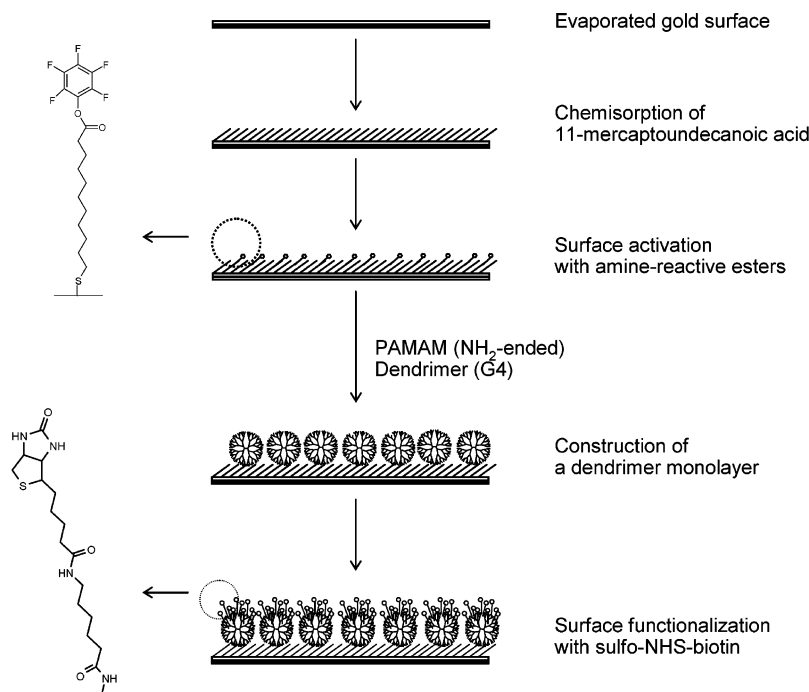
**Surface Characterization.** FT-IR spectroscopy and ellipsometry were performed to verify the formation of dendrimer monolayers on 11-MUA SAMs/Au. FT-IR spectra were recorded using a FT-IR spectrometer (Thermo Nicolet, NEXUS) equipped with a single-bounce attenuated total reflectance setup. *p*-Polarized light was reflected off the surface at an 80° angle. An average of more than 100 scans was taken to yield a spectrum at a resolution of 2

- (9) (a) Tokuhisa, H.; Kubo, T.; Koyama, E.; Hiratani, K.; Kanetsato, M. *Adv. Mater.* **2003**, *15*, 1534–1538. (b) Hong, M.-Y.; Lee, D.; Yoon, H. C.; Kim, H.-S. *Bull. Korean Chem. Soc.* **2003**, *24*, 1197–1202. (c) Snejdarkova, M.; Svobodova, L.; Nikolelis, D. P.; Wang, J.; Hianik, T. *Electroanalysis* **2003**, *15*, 1185–1191.
- (10) (a) Yoon, H. C.; Yang, H.; Kim, Y.-T. *Analyst* **2002**, *127*, 1082–1087. (b) Yoon, H. C.; Hong, M.-Y.; Kim, H.-S. *Anal. Chem.* **2000**, *72*, 4420–4427. (c) Yoon, H. C.; Kim, H.-S. *Anal. Chem.* **2000**, *72*, 922–926.
- (11) (a) Angenendt, P.; Glöckler, J.; Sobek, J.; Lehrach, H.; Cahill, D. J. *J. Chromatogr., A* **2003**, *1009*, 97–104. (b) Le Berre V.; Trévisiol, E.; Dagkessamanskaia, A.; Sokol, S.; Caminade, A. M.; Majoral, J. P.; Meunier, B.; François, J. *Nucleic Acids Res.* **2003**, *31*, e88. (c) Benters, R.; Niemeyer, C. M.; Drutschmann, D.; Blohm, D.; Wöhrle, D. *Nucleic Acids Res.* **2002**, *30*, e10. (d) Benters, R.; Niemeyer, C. M.; Wöhrle, D. *Chem. Biol. Chem.* **2001**, *2*, 686–694.
- (12) Uppuluri, S.; Keinath, S. E.; Tomalia, D. A.; Dvornic, P. R. *Macromolecules* **1998**, *31*, 4498–4510.

(13) Wells, M.; Crooks, R. M. *J. Am. Chem. Soc.* **1996**, *118*, 3988–3989.

(14) Frey, B. L.; Corn, R. M. *Anal. Chem.* **1996**, *68*, 3187–3193.

### Scheme 1. Bottom-Up Synthetic Procedures for Construction of Dendrimer Monolayers and Surface Functionalization with Biotin Ligands



cm<sup>-1</sup>. The thickness of the film was determined from an ellipsometer (Gaertner L116s) equipped with a He–Ne laser (632.8 nm) in air with a 70° angle of incidence at 632.8-nm wavelength. Film thicknesses of the dendrimer monolayers on the 11-MUA SAMs were calculated based on a refractive index of 1.46 for dendrimers and *n*-alkanethiols as reported by the Crooks group.<sup>15</sup> At least five different locations in each sample were measured and averaged.

The total density of functional amine groups at the interfacial layer was measured by a UV–visible spectrophotometer and through the use of the 4-NB molecule, which is comparable in size to biotin.<sup>16</sup> As previously demonstrated by Park and our groups, the 4-NB molecules completely attach to all amine groups on the surface via imine coupling, and release of the molecules can be attained through acid hydrolysis. Accordingly, the surface density of modifiable amine groups through the use of the 4-NB molecule was estimated by spectroscopic titration of acid-hydrolyzed 4-NB at 265-nm wavelength and calculated based on the extinction coefficient ( $\epsilon_{\text{max}} = 1.45 \times 10^4 \text{ M}^{-1} \cdot \text{cm}^{-1}$  in water or 0.2% acetic acid).

**SPR Measurements.** A BIAcore-X equipment was used for all SPR measurements with a flow rate of 3  $\mu\text{L}/\text{min}$ . The gold surface of a commercialized SPR sensor chip (SIA Kit Au, BIAcore AB) was briefly cleaned with 0.1 M NaOH solution containing 1% Triton-X 100. Each interfacial layer was constructed on the sensor chip according to the procedures mentioned above. The reagent for biotin functionalization was freshly prepared by mixing an aqueous solution of sulfo-NHS-biotin with the same volume of 0.1 M bicarbonate buffer (pH 9.5). The biotinylation reaction was

performed in two different ways: First, the surface was treated with a biotin reagent of 1 mg/mL, which had been confirmed to generate optimal binding of avidin.<sup>6</sup> Second, the surface was treated three times with a reagent of >5 mg/mL to create a fully biotinylated condition, as reported elsewhere.<sup>6</sup> The biotinylated surface was incubated with a NaOH solution (10 mM, pH ~12) for 30 min to remove succinimide byproducts adsorbed on the surface, as noted by Frey and Corn.<sup>14</sup>

For the SA binding reaction, a solution of SA (50  $\mu\text{g}/\text{mL}$  in PBST) was allowed to flow over the biotinylated surface. The SPR angle shift triggered by the association of SA was measured following washing with PBST for 10 min. Nonspecific adsorption of SA was also examined by running a SA solution (50  $\mu\text{g}/\text{mL}$  in PBST) prereacted with 1 mM biotin. A binding isotherm of SA was obtained by plotting the saturation coverage of SA as a function of the SA concentration in the bulk solution, where the protein concentration increased from 10 ng/mL to 50  $\mu\text{g}/\text{mL}$ . A reaction time was fixed in 30 min, by which the binding rate of SA lowered to a negligible level and the amount of bound SA was almost saturated. The increase of the SPR response was recorded after proper washing with PBST, and then the calculated surface coverage of SA was plotted as a function of the SA concentration in solution.

**Analysis of Binding Isotherms.** As described above, the saturation level of SA binding was measured following surface washing with a protein-free buffer solution, which gives the unequilibrium situation of irreversible SA binding. Under the continuous stream of SA solution (50  $\mu\text{g}/\text{mL}$  in PBST) prior to the washing step, however, the SPR responses induced by SA binding decreased only slightly after change into the flow of PBST buffer. Thus, to characterize the interaction of SA onto a biotinylated surface, we attempted to fit experimentally obtained binding data from the dendrimer layers to a simple Langmuir isotherm.

(15) Tokuhisa, H.; Zhao, M.; Baker, L. A.; Phan, V. T.; Dermody, D. L.; Garcia, M. E.; Peez, R. F.; Crooks, R. M.; Mayer, T. M. *J. Am. Chem. Soc.* **1998**, *120*, 4492–4501.

(16) Moon, J. H.; Kim, J. H.; Kim, K.; Kang, T.-H.; Kim, B.; Kim, C.-H.; Hahn, J. H.; Park, J. W. *Langmuir* **1997**, *13*, 4305–4310.

The analysis was carried out based on the assumptions that each binding site acts independently of other sites and the association of SA with a fully biotinylated surface proceeds entirely via bivalent binding.<sup>17</sup> In this regard, the bivalent binding model takes on the same general form as the monovalent model, and the binding data could be fit to the following Langmuir equation. The surface fractional coverage of protein is calculated using the saturation function as described elsewhere:<sup>18</sup>

$$\theta = \frac{\Gamma}{\Gamma_{\max}} = \frac{K[P]}{1 + K[P]}$$

where  $\theta$  is the surface fractional coverage of bound protein,  $\Gamma_{\max}$  is the surface concentration of protein at the full monolayer coverage,  $K$  is the apparent binding constant, and  $\Gamma$  is the surface concentration of associated proteins when the bulk concentration of protein is  $[P]$ . A linear plot of the experimentally determined  $\theta^{-1}$  as a function of  $[P]^{-1}$  yields the value of the binding constant,  $K$ .

## RESULTS AND DISCUSSION

**Construction of Interfacial Layers.** Uniformity and homogeneity of an interfacial layer are prerequisite for the characterization of binding kinetics of SA on a biotin-functionalized surface. With the use of PAMAM dendrimers from plateletlike G1 to globular-shaped G4 (~4.5 nm), of which the structural and physical properties are summarized in Table S1 (see Supporting Information), it was possible to construct a complete, even layer of dendrimer molecules in a molecularly organized manner on gold. Previously, characterization of the dendrimer monolayers by using various analytical tools revealed that the packing density of the dendrimer molecule or the surface density of functional groups is quite different depending on the generation number of the dendrimer.<sup>10b,13,15</sup> In this study, we employed chain-end amine groups of the dendrimer for functionalization of biotin with the exception of its layer formation. Thus, we first examined formation of the dendrimer monolayers and the relative densities of the functional amine groups at their surfaces. As shown in Scheme 1, bottom-up synthetic procedures for preparation of dendrimer monolayers were clearly elucidated by the Crooks group.<sup>13</sup> Following covalent attachment of the dendrimer onto an amine-reactive surface, the peaks between 1720 and 1740  $\text{cm}^{-1}$ , derived from 11-MUA carbonyl groups, disappeared. Amide I and II bands were observed at 1660 and 1560  $\text{cm}^{-1}$ , respectively. Relative intensities of the amide bands confirmed the dendrimer monolayer with different generation numbers on gold (Figure 1A). A thickness of the dendrimer layer increased with the generation number of the dendrimer (Figure 1B). However, the measured thickness was quite smaller than the bulk-phase diameter of the dendrimer itself due to substantial distortion of the dendrimer when immobilized on a surface, as noted by Tokuhisa et al.<sup>15</sup> This observation has previously been examined by Crooks and our groups; the monolayer of a ferrocene-tethered G4 dendrimer was prepared on gold, and the surface mole fraction of the immobilized

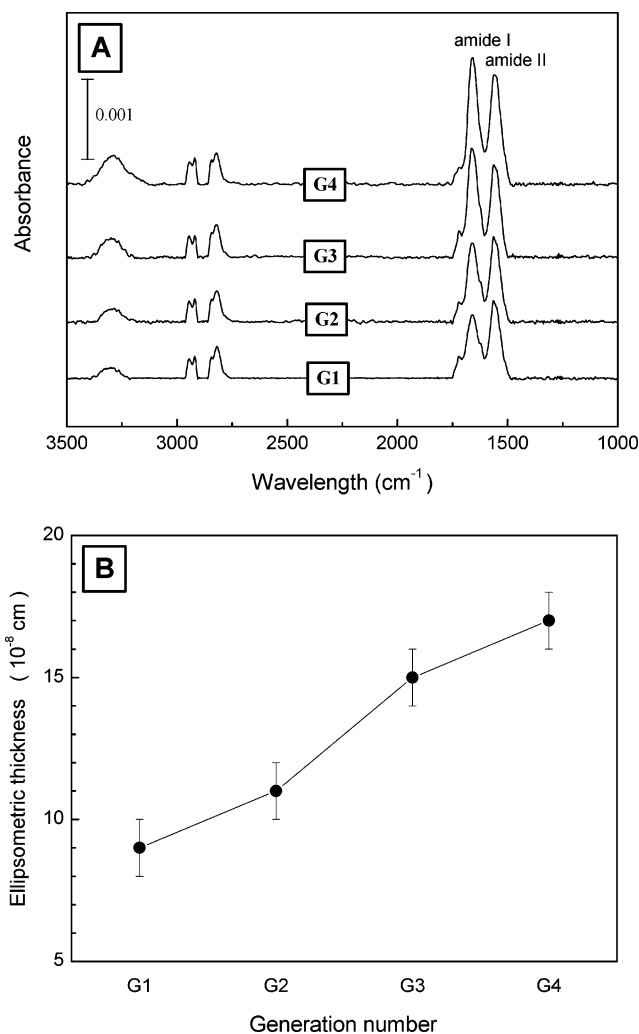


**Figure 1.** FT-IR spectra (A) and ellipsometric thicknesses (B) obtained from the dendrimer monolayers, which are covalently attached to activated 11-MUA SAMs on gold.

dendrimer was estimated from the electrochemical titration of electroactive ferrocene moieties. Due to surface immobilization of the dendrimers with significant deformation, the mole fraction of the dendrimer in its monolayer form was measured to be 270–280% of the full monolayer coverage calculated from its bulk dimension.<sup>10b,15</sup> Based on these circumstances, the surface analysis performed in this study clearly indicates the formation of complete, even dendrimer monolayers on gold as reported elsewhere.<sup>10,13,15</sup> For comparison, 11-MUAmine SAMs and a PLL layer presenting functional amine groups were employed. SAMs and layers of linear polymers have been commonly used for kinetic studies of protein–ligand interactions. In particular, the SA–biotin interaction has been well studied on biotin-containing mixed SAMs regarding kinetics of protein adsorption and the binding efficiency of protein.<sup>2</sup> As for the PLL layer, Frey and Corn reported that a linear polymer with a helixlike conformation lies parallel to a surface in an extended configuration when covalently attached to an activated surface.<sup>14</sup> Thus, a similar thickness of  $10 \pm 2 \text{ \AA}$  was observed from the monolayers of commercially available PLLs with shorter or longer chain lengths, resulting in the same amounts of bound avidin. Based on known facts from well-defined systems, we reasoned that comparative analyses of the aforemen-

(17) (a) Smith, E. A.; Thomas, W. D.; Kiessling, L. L.; Corn, R. M. *J. Am. Chem. Soc.* **2003**, *125*, 6140–6148. (b) Yang, T.; Baryshnikova, O. K.; Mao, H.; Holden, M. A.; Cremer, P. S. *J. Am. Chem. Soc.* **2003**, *125*, 4779–4784.

(18) Pisarchick, M. L.; Thompson, N. L. *Biophys. J.* **1990**, *58*, 1235–1249.

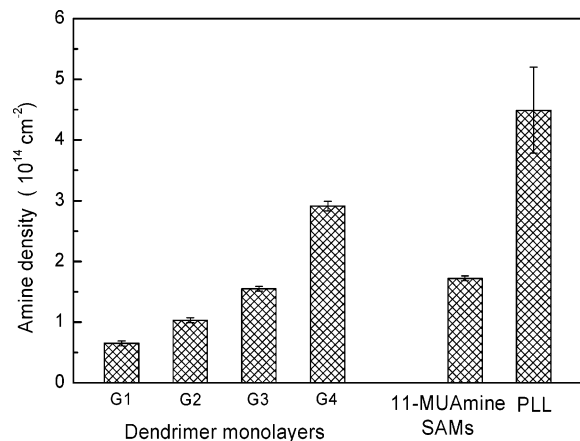


**Figure 2.** Surface densities of modifiable amine groups.

tioned interfacial layers may reveal unique characteristics of dendrimer monolayers, which induce an efficient SA–biotin interaction.

Following the construction of respective interfacial layers on gold, the resulting surface was functionalized with biotin and then subjected to the SA binding reaction. To examine the interaction of SA on interfacial layers with different biotin densities, the surface density of functionalized biotin was estimated indirectly from the density of modifiable amine groups at each surface. Since the 4-NB molecule has the ability to attach to all amine groups on a surface and has a size similar to biotin, the surface densities of modifiable amine groups by 4-NB can be used to compare the relative densities of functionalized biotin among tested layers. The amount of modifiable amine groups was measured from the spectroscopic titration of acid-hydrolyzed 4-NB following imine coupling, as reported elsewhere.<sup>16</sup> It has also been confirmed that the coupling of 4-NB was no longer detected on the fully biotinylated surface.<sup>6</sup> Accordingly, it seems reasonable that the maximum density of functionalized biotin at each surface can be predicted from the surface density of modifiable amine groups by 4-NB. As shown in Figure 2, the 11-MUAmine SAMs revealed an amine density of  $(1.7 \pm 0.04) \times 10^{14} \text{ cm}^{-2}$ . This corresponds to  $\sim 57\text{--}71\%$  of the ferrocene density averages of  $(2.4\text{--}3.0) \times 10^{14} \text{ cm}^{-2}$ , which were electrochemically measured on the SAMs of ferrocene (6.6-Å diameter)-terminated alkanethiols on gold.<sup>19</sup> While the amine densities of the G1 and G2 layers were lower than the 11-MUAmine SAMs, the G3 layer showed a similar amine density. The G4 layer especially showed nearly a 2-fold higher amine density than the G3 layer and 11-MUAmine SAMs. The probable cause of this increase in density seems to be the increased packing density of the molecule due to substantial distortion of the G4 dendrimer when immobilized on the surface.<sup>6,10b,15</sup> An amine density of the PLL layer was observed to be the highest, showing a  $\sim 1.5$ -fold higher level than the G4 layer.

**Streptavidin Binding Reaction.** Variation of SA binding levels has been well studied on biotin-containing SAMs of alkanethiols as a function of the surface mole fraction and orientation of biotin ligands.<sup>2,4,5</sup> As a result, it has been revealed that the interaction of SA is mainly triggered by the presence of biotin on a surface. It was also found that the SA binding level sharply increased as a function of the biotin density until a biotin concentration of 5%.

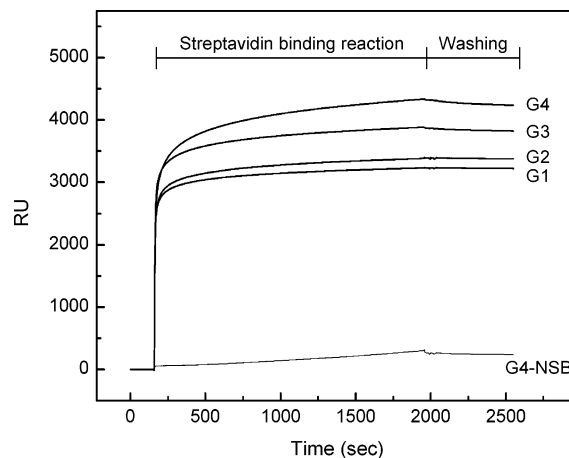


**Figure 3.** SPR sensorgrams for the interaction of SA onto a biotinylated surface. Sensorgrams (G1–G4) show the RU changes when a SA solution ( $50 \mu\text{g/mL}$  in PBST) was allowed to flow over a biotinylated surface. A sensorgram at the bottom (G4-NSB) displays the RU change when the biotinylated G4 layer was reacted with a SA solution presaturated with 1 mM biotin.

The maximum level of  $\sim 2.4 \text{ ng}\cdot\text{mm}^{-2}$  was then maintained up to a biotin concentration of  $\sim 50\%$ .<sup>2,5,20</sup> Further increase in a biotin concentration was likely to adversely affect the SA binding level. This outcome was explained by unfavorable steric interactions among highly occupied biotin moieties and incoming SA molecule or by the poor orientation of functionalized biotin.<sup>2,5</sup> In contrast, our previous study showed that the G4 layer facilitated an efficient SA–biotin interaction even at higher biotin concentrations, resulting in an avidin binding level of  $\sim 5.0 \pm 0.2 \text{ ng}\cdot\text{mm}^{-2}$ , which represents a hexagonal-like arrangement of SA.<sup>6</sup> In the present study, we attempted to assess the dependency of the optimum binding level of SA on the surface structure of the interfacial layer to elucidate unique features of the SA–biotin interaction on dendrimer layers. To this end, the optimal binding level of SA was compared among different surfaces that were treated with a biotin reagent of 1 mg/mL (Figure 3; Figure S1, see Supporting Information). Previously, we found that the surface functionalization with a biotin reagent of 1 mg/mL resulted in sufficient biotin densities for optimal binding of avidin for dendrimer and PLL layers.<sup>6</sup> However, it is anticipated that the biotin densities may vary widely among the tested layers even following functionalization of biotin under the same conditions. Thus, the effect of biotin density on the maximum binding level of SA was independently confirmed for each surface. By reacting three times with a biotin reagent of  $\sim 5 \text{ mg/mL}$ , each interfacial layer was fully functionalized to give rise to the maximum biotin density, which had been previously confirmed by our group.<sup>6</sup> The resulting surface was then subjected to a SA binding reaction. The amount of bound SA measured from SPR analysis was converted to the surface coverage of SA. Based on the assumption that a mass change of  $1 \text{ ng}\cdot\text{mm}^{-2}$  in a SPR sensorgram corresponds to the resonance angle shift of  $0.1^\circ$  at a sensing surface,<sup>21</sup> the surface fractional coverage of protein was calculated by dividing the experimentally measured value ( $\text{ng}\cdot\text{mm}^{-2}$ ) by a theoretical estimate of the

(20) Zhao, S.; Reichert, W. M. *Langmuir* **1992**, *8*, 2785–2791.

(21) Stenberg, E.; Persson, B.; Ross, H.; Urbaniczky, C. J. *Colloid Interface Sci.* **1991**, *143*, 513–526.

(19) Finklea, H. O. *Electroanal. Chem.* **1996**, *19*, 109–335.

**Table 1. Levels of Specific Binding and Nonspecific Adsorption of Streptavidin<sup>a</sup>**

surfaces		biotinylated with 1 mg/mL reagent		fully biotinylated condition		
		SA bound (ng·mm <sup>-2</sup> )	surface coverage (%)	SA bound (ng·mm <sup>-2</sup> )	surface coverage (%)	nonspecific adsorption <sup>b</sup> (%)
dendrimer monolayer	G1	3.2 ± 0.1	63 ± 2	3.3 ± 0.2	65 ± 4	1.4 ± 0.3
	G2	3.6 ± 0.1	71 ± 2	3.6 ± 0.2	71 ± 4	1.6 ± 0.5
	G3	4.0 ± 0.1	79 ± 2	4.0 ± 0.3	79 ± 6	3.0 ± 2.0
	G4	4.3 ± 0.1	87 ± 2	4.2 ± 0.1	83 ± 2 (100) <sup>c</sup>	5.0 ± 1.0
SAMs: ratio of 11-MUAmine to 11-MU-ol	1.0			2.4 ± 0.2	47 ± 4 (57)	1.3 ± 0
	0.5			2.3 ± 0.1	45 ± 2	1.0 ± 0.2
	0.1			2.3 ± 0.1	45 ± 2	1.0 ± 0.2
Poly(L-lysine) layer			2.8 ± 0.1	55 ± 2 (67)	1.6 ± 0	

<sup>a</sup> Each reported value represents at least four assays. <sup>b</sup> Relative level to specific binding of SA. <sup>c</sup> Relative value to the amount of bound SA at a G4 dendrimer monolayer.

maximum amount of protein, given that the protein molecules are closely packed in a hexagonal arrangement.<sup>22</sup> In this case, the theoretical monolayer coverage of bound protein per unit surface area was estimated using the equation,  $[(10^{14}/\pi r^2)/(10^{-9}N_A/MW)]$ , where  $r$ ,  $MW$ , and  $N_A$  correspond the radius and molecular weight of a molecule and Avogadro's number, respectively. A mean value of the radius (25 Å) was obtained from the molecular dimension ( $\sim 4.5 \times 4.5 \times 5.8$  nm) of SA.<sup>2c</sup>

The estimated protein surface coverages for the optimal binding levels of SA are listed in Table 1. In accordance with our previous result, the G4 layer showed the highest SA coverage of  $\sim 87\%$ , and the PLL layer and 11-MUAmine SAMs were estimated to exert 67 and 57% of the highest SA coverage from the G4 layer, respectively.<sup>6</sup> On most surfaces, optimal binding of SA was observed when the surface was functionalized with a biotin reagent of 1 mg/mL or fully biotinylated. As for the G4 layer, the use of a 1 mg/mL biotin reagent exhibited a slightly higher SA coverage (87%) than the fully biotinylated condition (83%). In the present study, it was observed that all dendrimer layers resulted in higher SA coverage than the PLL layer and 11-MUAmine SAMs. As the dendrimer molecule changed from the extended, platelike G1 to the closed, spheroidlike G4, the SA coverage increased from about 67 to 87%, approaching a theoretical maximum coverage of 90.7% for the adsorption of protein on a planar surface.<sup>23</sup> According to the geometric simulation of protein adsorption, a full monolayer coverage of protein can be ideally attained when protein molecules are immobilized on a surface in a hexagonal arrangement. The PLL layer and 11-MUAmine SAMs led to about 55 and 46% SA coverages around the maximum surface coverage (54.7%) attainable by the random sequential adsorption (RSA) of protein, as reported elsewhere.<sup>23,24</sup> In all cases, nonspecific binding of SA was less than 5% compared to specific binding levels (Figure 3; Figure S1, see Supporting Information).

To confirm the optimum binding of SA onto the 11-MUAmine SAMs, mixed SAMs with different amine densities were constructed by reacting the solution with various ratios of 11-

MUAmine to 11-MU-ol (0.1, 0.5, and 1.0) and fully functionalizing with biotin. Like other tested systems, preparation of 11-MUAmine SAMs on gold was conducted prior to functionalization of biotin and then subjected to a SA binding reaction. SPR analysis revealed that the amounts of bound SA ranged from 2.3 to 2.4 ng·mm<sup>-2</sup> regardless of the ratio of surface amine functionalities (i.e., the surface density of biotin) (Table 1), which was almost identical to reported data.<sup>2</sup> In the studies performed by Jung et al., which were based on mixed SAMs incorporating biotinylated thiols, the optimum binding level of SA was maintained at  $\sim 2.4$  ng·mm<sup>-2</sup> when the biotin densities ranged from  $0.4 \times 10^{14}$  to  $1.6 \times 10^{14}$  cm<sup>-2</sup>.<sup>2a</sup> They also reported that single-component SAMs of biotinylated thiols represented a maximum biotin density of  $\sim 4.0 \times 10^{14}$  cm<sup>-2</sup>. Given that the ratio of 11-MUAmine to 11-MU-ol on the surface is identical to its ratio in the reaction solution and that the amine groups of prepared SAMs are fully biotinylated under the given experimental condition, biotin densities obtained from the mixed SAMs of 11-MUAmine and 11-MU-ol were approximated to be 4–43% of the maximum biotin density measured by Jung et al. In the case of fully biotinylated G1–G3 layers, the measured biotin densities were also found to be within the range that resulted in optimal binding of SA. Even in the context of optimal biotin densities, the dendrimer layers from G1 to G3 exhibited much higher SA coverages than the tested SAMs. Interestingly, the fully biotinylated G4 layer maintained a SA coverage at 83% under the condition where the predicted biotin density of  $(2.9 \pm 0.08) \times 10^{14}$  cm<sup>-2</sup> was fairly higher than the optimal range of biotin densities. SA coverage of the PLL layer was limited to  $\sim 67\%$  of the G4 layer despite a 1.5-fold higher biotin density. Based on the observations with respect to the optimal binding of SA at various layers, it is likely that the maximum surface coverage of SA is profoundly affected by the surface structure of an underlying interfacial layer rather than the surface density of biotin.

**Binding Kinetics of Streptavidin.** Kinetics of the adsorption/desorption of SA on biotin-containing mixed SAMs have been studied as a function of the surface mole fraction of a biotinylated thiol to explicitly explain binding behavior of SA to a surface with a defined composition.<sup>25</sup> Adsorption/desorption kinetics of SA was examined by employing engineered SAs with reduced affinity for biotin, since an irreversible binding system with highly strong

(22) Lahiri, J.; Isaacs, L.; Tien, J.; Whitesides, G. M. *Anal. Chem.* **1999**, *71*, 777–790.

(23) Roth, C. M.; Lenhoff, A. M. In *Biopolymers at Interfaces*; Malmsten, M. Ed.; Marcel Dekker: New York, 1998; pp 89–118.

(24) (a) Feder, J. J. *Theor. Biol.* **1980**, *87*, 237–254. (b) Feder, J.; Giaever, I. J. *Colloid Interface Sci.* **1980**, *78*, 144–154.

**Table 2. Binding Kinetics of Streptavidin on Biotinylated Surfaces<sup>a</sup>**

surfaces		biotinylated with 1 mg/mL reagent		fully biotinylated condition	
		init binding rate <sup>b</sup> ( $10^{11}$ molecules·cm <sup>-2</sup> ·s <sup>-1</sup> )	$T_{\theta/2}$ (s)	init binding rate ( $10^{11}$ molecules·cm <sup>-2</sup> ·s <sup>-1</sup> )	$T_{\theta/2}$ (s)
dendrimer monolayer	G1	2.5 ± 0.1	6.0	2.3 ± 0.2	7.5
	G2	2.7 ± 0.1	6.0	2.3 ± 0.3	7.5
	G3	2.8 ± 0.2	6.5	2.5 ± 0.4	8.0
	G4	2.8 ± 0.3	7.5	2.4 ± 0.3	8.0
SAM: ratio of 11-MUAmine to 11-MU-ol	1.0	-	-	1.2 ± 0.1	9.5
	0.5	-	-	1.0 ± 0.2	11.0
	0.1	-	-	1.1 ± 0.1	10.0
poly(L-lysine) layer	-	-	2.5 ± 0.2	5.5	

<sup>a</sup> Each reported value represents at least four assays. <sup>b</sup> The amount of bound SA by a 10-min reaction is defined as the saturation coverage ( $\theta$ ) and the elapsed time to reach  $\theta/2$  as  $T_{\theta/2}$ , respectively. The initial binding rate of SA is calculated by dividing  $\theta/2$  by  $T_{\theta/2}$ . In this case, the obtained ' $\theta$  (ng·mm<sup>-2</sup>)' from SPR measurements was converted into the number of bound SA molecules per centimeter squared.

interaction is not amenable to the estimation of  $k_{on}$  and  $k_{off}$ . To compare binding kinetics of SA with wild type and mutant, the initial binding rate of SA was determined from an experimentally obtained SPR sensorgram.<sup>2a</sup> In this notion, the amount of bound SA during a 10-min reaction is denoted as the saturation coverage ( $\theta$ ) and the elapsed time to reach  $\theta/2$  as  $T_{\theta/2}$ . Accordingly, the initial binding rate of SA is calculated by dividing  $\theta/2$  by  $T_{\theta/2}$ . In the present study, binding kinetics of wild-type SA was evaluated as a function of the surface structure of an interfacial layer. From obtained SPR sensorgrams,  $T_{\theta/2}$  values were measured to be 5–8 s for dendrimer and PLL layers and 9–11 s for SAMs. Using the same approach as Jung et al., the initial binding rates of SA were calculated and given in Table 2. Mixed SAMs of 11-MUAmine and 11-MU-ol revealed an initial binding rate of SA  $\sim(1.1 \pm 0.2) \times 10^{11}$  molecules·cm<sup>-2</sup>·s<sup>-1</sup> regardless of the density of functionalized biotin. These estimates were found to be within the range of measured values from the interaction of SA onto biotin-containing SAMs.<sup>2a</sup> Interestingly, all dendrimer layers showed nearly 2-fold higher initial binding rates of SA than the SAMs independently of the surface density of biotin. Even in the context of much higher biotin densities than the optimal range, the G4 layer gave rise to a 2-fold faster binding rate of SA. Like the dendrimer layers, the PLL layer generated 2-fold higher rates for initial binding of SA. As stated earlier, a maximum SA coverage of the PLL layer was restricted to  $\sim 67\%$  of the G4 layer despite a 1.5-fold higher biotin density. The PLL layer is expected to display an irregular surface following covalent attachment of the PLL molecule with a helixlike polypeptide structure on a surface. When considering that the surface-exposed portion of functionalized biotin is generally amenable to the interaction with SA, the above observations indicate that the interactions of SA onto the biotinylated dendrimer layers, including the PLL layer, are quite different from those of the SAMs. This also implies that binding kinetics of SA, together with the saturation protein coverage, is entirely dependent on the surface structure of an underlying interfacial layer.

The sticking probability is defined as the probability of a molecule to adsorb onto a surface upon collision, and this reflects

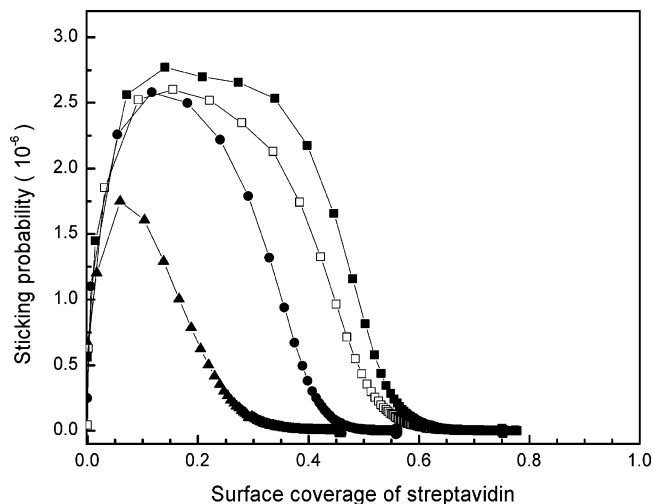


**Figure 4.** Variation of the sticking probability as a function of the surface coverage of SA on biotinylated surfaces; PAMAM G3 dendrimer monolayer (■), PAMAM G1 dendrimer monolayer (□), poly(L-lysine) layer (●), and 11-MUAmine SAMs (▲).

the difficulty in overcoming the free energy barrier for adsorption. To characterize the SA–biotin interaction on a surface, Jung et al. first introduced the notion of sticking probability in the adsorption of protein from a liquid solution, and its variation was traced as the surface coverage of protein increased.<sup>2a,25</sup> To understand in more detail SA binding processes on dendrimer layers, a maximum sticking probability and its duration were monitored as a function of the surface coverage of SA. The obtained results from different surfaces were compared with the predicted profile from mixed SAMs by Jung et al.<sup>2a</sup> The sticking probability is calculated by dividing the binding rate of SA by the collision frequency,  $C_s[k_B T / (2\pi m)]^{1/2}$ .<sup>26</sup> In this equation,  $C_s$ ,  $k_B$ , and  $m$  represent the concentration of SA nearest the surface, Boltzmann's constant, and the mass of SA, respectively. Jung et al. conducted the SA binding reaction in a batch reaction system using a home-built SPR instrument equipped with a stop flow system and predicted  $C_s$  versus time using a finite-difference numerical method.<sup>2a</sup> Under the static flow of a SA solution with a concentration of 50  $\mu\text{g/mL}$ , it was defined that the adsorption rate of SA was nearly diffusion-limited. In this work, a commercialized BIAcore instrument was employed, which continuously delivers a protein solution of constant concentration through a microfluidic device. It was thus assumed that  $C_s$  is identical to the bulk concentration of SA (50  $\mu\text{g/mL}$ ). Accordingly, variation of the sticking probability has the same tendency as that of the SA binding rate as the surface coverage of SA increases.

The change in sticking probability with respect to the surface coverage of SA at different surfaces can be seen in Figure 4. From a starting point on the  $x$  axis, the increase in measured data at the lowest protein coverages was probably due to the slow response time of a flow system, as noted by Jung et al.<sup>2a</sup> As a general trend, the sticking probability increased sharply at the beginning of the binding process, reached a maximum level, and then radically declined as the SA coverage increased. At a SA coverage of 0.15, the sticking probabilities of SA from the

(25) Jung, L. S.; Campbell, C. T. *J. Phys. Chem. B* **2000**, *104*, 11168–11178.

(26) Jung, L. S.; Campbell, C. T. *Phys. Rev. Lett.* **2000**, *84*, 5164–5167.

dendrimer and PLL layers reached a plateau around  $2.7 \times 10^{-6}$ , yielding a SA density of  $7.6 \times 10^{11}$  molecules·cm<sup>-2</sup>. A maximum probability of the dendrimer layers was ~1.5-fold higher than the peak value observed from the 11-MUAmine SAMs. This increase is consistent with the elevation of the initial binding rates of SA. Among the tested surfaces, the G3 layer displayed the highest probability at a fixed SA coverage and retained the maximum probability up to a SA coverage of 0.35, which corresponds to a SA density of  $1.8 \times 10^{12}$  molecules·cm<sup>-2</sup>. Likewise, a similar variation of sticking probability was observed at the G4 layer (Figure S2, see Supporting Information). The G1 layer exhibited a profile analogous to the G3 layer although the probabilities were slightly lower than the G3 layer. On the other hand, the 11-MUAmine SAMs gave rise to a rather different profile of sticking probability with respect to the SA coverage when compared with those of the dendrimer and PLL layers. A peak probability of  $1.8 \times 10^{-6}$  was observed around a surface coverage of 0.06. Thereafter, the probability rapidly decreased and ultimately reduced to a negligible level above a SA coverage of 0.4. This variation is very similar to the predicted profile from biotin-containing mixed SAMs studied by Jung et al.,<sup>2a</sup> but observed data at a fixed protein coverages in our tested systems were less than the reported ones. As stated earlier, the discrepancy in the estimated probability seemed to be caused by the definition of  $C_s$  depending on the static or continuous flow of SPR-sensing instruments.

From quantitative modeling of SA binding onto biotin-containing SAMs, it has been shown that steric interactions among preoccupied molecules significantly prevent the adsorption of protein from exceeding a jamming limit of the RSA process as well as from approaching a theoretical monolayer coverage in a hexagonal packing of protein.<sup>23,24</sup> Thus, the RSA process of protein limits a maximum protein coverage below the jamming limit (54.7%). For this reason, we presumed that the extent of lateral steric hindrance on dendrimer layers would be represented by variation of sticking probability as the surface coverage of SA increases. As a result, the dendrimer layers were found to maintain significant levels around a maximum probability for a longer period. With this, it is likely that the surface structure of the dendrimer monolayers made a significant contribution to minimizing the lateral steric hindrance, consequently enhancing protein coverage up to a theoretical maximum level. Among the traits of the dendrimer molecule in solution and its monolayer reported elsewhere,<sup>6,10,12,13,15,27</sup> it is noteworthy that key factors responsible for an efficient SA–biotin interaction with highly ordered packing would be surface distribution of the chain-end amine groups of the dendrimers for functionalization of biotin, surface corrugation of the dendrimer layers, and flexibility of highly branched larger dendrimers. Under our experimental conditions, dendrimer layers with sufficient biotin densities for optimal binding of SA would undergo bivalent binding of SA with surface-functionalized biotin. The exceptionally high binding affinity of SA for biotin ( $K_a \sim 10^{13}$  M<sup>-1</sup>) via bivalent binding would lead to the instantaneous and irreversible adsorption of SA on the surface. Consequently, migration of bound SA molecules might be extremely rare. Under these circumstances, the earlier association of SA onto most of the tested surfaces, giving low protein coverages less than 0.1, would not be affected substantially by unfavorable steric interac-

tions among preoccupied SA molecules, in which condition all dendrimer layers exhibited fairly faster binding of SA than the SAMs (Figure 4). This finding implies that surface distribution of functionalized biotin on the dendrimer layers might play a central role in the facile interaction of SA. As surface coverage of SA increased in our tested surfaces with optimal biotin densities, underlying environments such as the surface display of functionalized biotin and the surface architecture of the interfacial layer would considerably influence the sequential process of SA binding. Governed by the random sequential adsorption of protein, it has been known that the randomness of the locations at which SA adsorbs results in a considerable fraction of uncovered surface with the excluded-area feature.<sup>23,24</sup> In contrast with SAMs, the dendrimer layers showed higher sticking probabilities up to a SA coverage of 0.4 (Figure 4). Remarkably, the corrugated surface of the G4 layer attained a hexagonal-like arrangement of SA, which is a 1.4-fold greater SA coverage than the G1 layer (Table 1). Of the key factors mentioned above, the surface corrugation and the flexibility of the immobilized dendrimer can be represented when globular-shaped and highly branched larger dendrimers (e.g., G3 and G4 in our systems) are immobilized on the surface. Globular shape of the dendrimer is likely to render its monolayer a quasi-three-dimensional surface, resulting in an increase of an effective surface area. In addition, the Cloninger group previously suggested that highly branched dendrimers are considered to be more flexible and can more effectively avoid unfavorable steric interactions than low-generation dendrimers when immobilized on the surface.<sup>27</sup> In a mixture of sample solutions, they systematically studied multivalent protein–carbohydrate interactions between mannose-modified dendrimer and concanavalin A (Con A) as a function of the number of sugars on the dendrimer and the generation of the dendrimer. As one of the results, it was noted that a maximum activity of Con A binding per mannose-modified dendrimer was slightly fallen off the calculated number of Con A that should fit around each dendrimer.<sup>27a</sup> As the cause of the skewing trend, they presumed that the additional Con A binding over the simulated value was ascribed to an increasing flexibility of dendrimer shape with increasing generation number and correspondingly increasing surface areas. Based on these considerations, it is plausible that, on biotinylated layers of high-generation dendrimers, the interposition of free SA molecules by slanting among preoccupied ones is possible as the SA is interacted in a random distribution. In conclusion, the surface corrugation in a few nanometers and more flexibility of larger dendrimers seems to be attributed to relieving the lateral steric effect and sustaining faster SA binding even with increasing SA coverage, yielding highly ordered packing of SA.

**Isotherms of SA Binding.** In contrast with SA coverages from the 11-MUAmine SAMs (46%) and PLL layer (55%), the G4 dendrimer layer resulted in a SA coverage of 87%, strongly implying a hexagonal-like distribution of SA on the surface. The hexagonal arrangement of protein might be possible in the absence of steric repulsion among adsorbed protein molecules, as stated earlier.<sup>23</sup> In this regard, we attempted to get some insight into the adsorption behavior of protein on dendrimer layers and

(27) (a) Woller, E. K.; Walter, E. D.; Morgan, J. R.; Singel, D. J.; Cloninger, M. *J. Am. Chem. Soc.* **2003**, *125*, 8820–8826. (b) Schlick, K. H.; Udelhoven, R. A.; Strohmeyer, G. C.; Cloninger, M. *J. Mol. Pharm.* **2005**, *2*, 295–301.

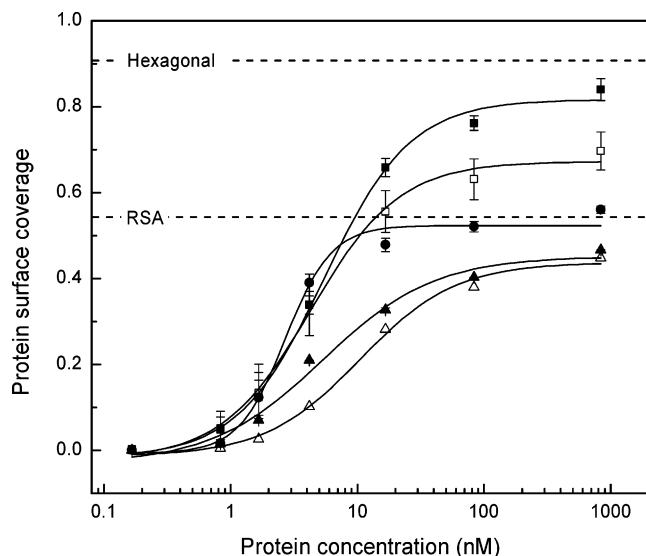


**Figure 5.** Isotherms for SA binding on biotinylated surfaces; PAMAM G3 dendrimer monolayer (■), PAMAM G1 dendrimer monolayer (□), poly(L-lysine) layer (●), 11-MUAmine SAMs (▲), and mixed SAMs of 11-MUAmine and 11-MU-ol (reaction ratio 1:9) (△). A solid line represents the best fit of the data as a guide to the eye.

the degree of lateral steric effect.<sup>17a,27,28</sup> Isotherms plotting the saturation coverage of SA as a function of the SA concentration in solution were obtained, and then the experimental data were fit to a Langmuir isotherm model, although all assumptions of the Langmuir model may not be valid for the adsorption of protein. The Langmuir isotherm model is based on the assumptions that adsorption takes place on discrete sites, all surface sites are equivalent, and adsorption to one site is independent of the occupancy of adjacent sites.<sup>23,29</sup>

Binding isotherms of SA showing the dependency of the SA coverage on the SA concentration in solution are presented in Figure 5. The dendrimer and PLL layers generated much steeper isotherms than the 11-MUAmine SAMs, displaying analogous profiles up to a SA concentration of ~10 nM. Afterward, the surfaces approached saturation coverages of SA in different paths. As for the 11-MUAmine SAMs, the SA coverage increased slowly up to a protein concentration of 17 nM and reached a saturation level below the jamming limit of a RSA model. Fits of the experimental data revealed that the binding behavior of SA on

the G1 and G3 layers closely follows the Langmuir model (Figure S3, see Supporting Information). From a linear plot of a Langmuir equation, the SA binding constant of the biotinylated surface was estimated to be  $7.3 \times 10^7 \text{ M}^{-1}$  for the G1 layer and  $7.6 \times 10^7 \text{ M}^{-1}$  for the G3 layer. This result also shows that the lateral steric effect was considerably minimized on the dendrimer monolayers even with increasing SA coverage.

## CONCLUSIONS

Based on the kinetic and equilibrium binding analyses of SA on biotinylated dendrimer monolayers, we demonstrated that unique surface features of the dendrimer monolayers resulted in relatively higher binding rates and saturation coverages of SA when compared with SAMs and a PLL layer. Typically, observed SA coverage from the G4 layer approached the theoretical maximum level that can be attained when the molecules are closely packed in a hexagonal arrangement. In kinetic studies, the initial binding rate of SA was nearly 2-fold higher in all dendrimer layers than in SAMs. Variation of the sticking probability versus the surface coverage of SA as well as the binding isotherms of SA provided evidence that the lateral steric effect was considerably minimized on the dendrimer layers even with increasing SA coverage. Accordingly, the binding behavior of SA on the G1 and G3 layers was well interpreted by a Langmuir model. The surface distribution of functionalized biotin, surface corrugation, and increasing flexibility of highly branched larger dendrimers seem to be the crucial aspects of dendrimer monolayers enabling an efficient SA–biotin interaction, which offers a guideline for the construction and analysis of an interfacial layer in biosensing applications.

## ACKNOWLEDGMENT

This work was supported by the National Research Laboratory Program and IMT-2000 of the MOST, the BK21 Program of the MOE, and Nano-Bio program of MOCIE, Korea. We thank I. S. Choi (Department of Chemistry, KAIST) for technical assistance and H. C. Yoon (Ajou Univ, Korea) for comments on the manuscript.

## SUPPORTING INFORMATION AVAILABLE

Additional information as noted in text. This material is available free of charge via the Internet at <http://pubs.acs.org>.

Received for review June 14, 2005. Accepted September 8, 2005.

AC051045R

(28) Zhao, S.; Walker, D. S.; Reichert, W. M. *Langmuir* **1993**, *9*, 3166–3173.

(29) Andrade, J. D. In *Surface and Interfacial Aspects of Biomedical Polymers*; Andrade, J. D., Ed.; Plenum Press: New York, 1985; pp 1–80.